Electronic Supplementary Material (ESI) for Soft Matter.

Supporting Information

Multi-stimuli-responsive chiral organogels based on peptide derivatives

Chang-Wei Liu, Ming Su, Xue-Liang Li, Teng Xue, Na Liu, Jun Yin, Yuan-Yuan Zhu, and Zong-Quan Wu**

School of Chemistry and Chemical Engineering, Key Laboratory of Advanced Functional Materials and Devices, Anhui Province, Hefei University of Technology, Hefei, Anhui, 230009, China.

E-mail: yyzhu@hfut.edu.cn; zqwu@hfut.edu.cn

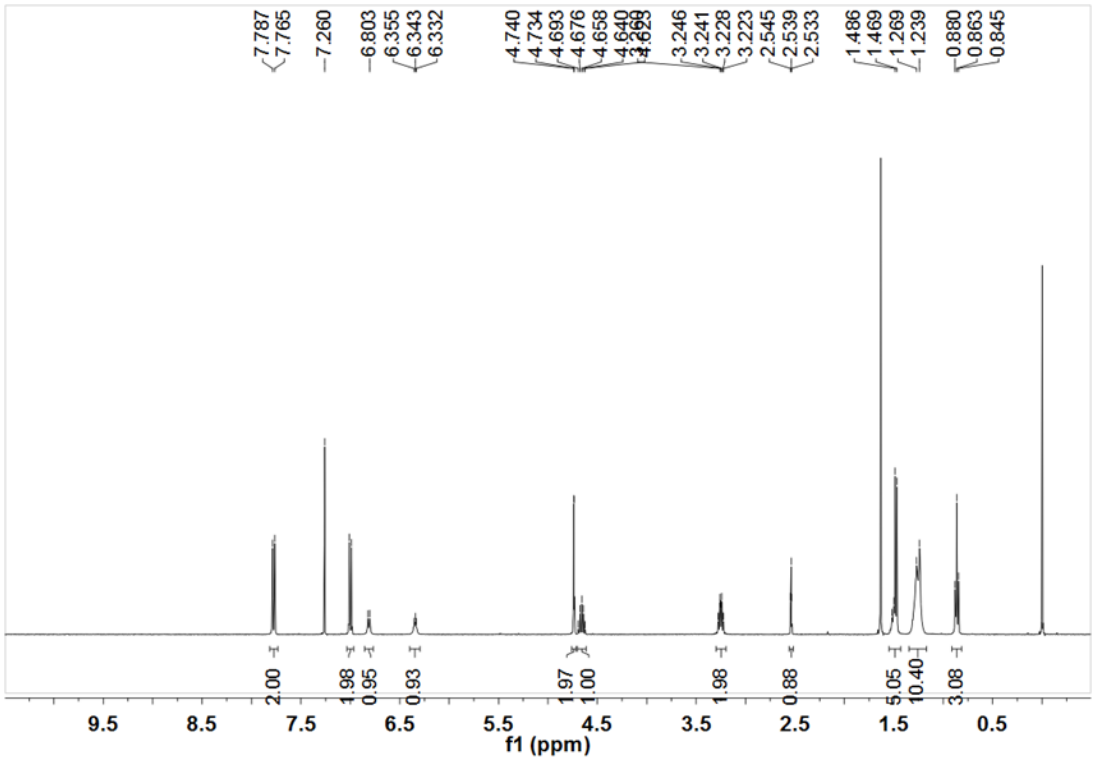

Figure S1. ^{1}H NMR spectrum of compound $\mathbf{1^{L}}$ (400 MHz) in $CDCl_3$ (10 mM).

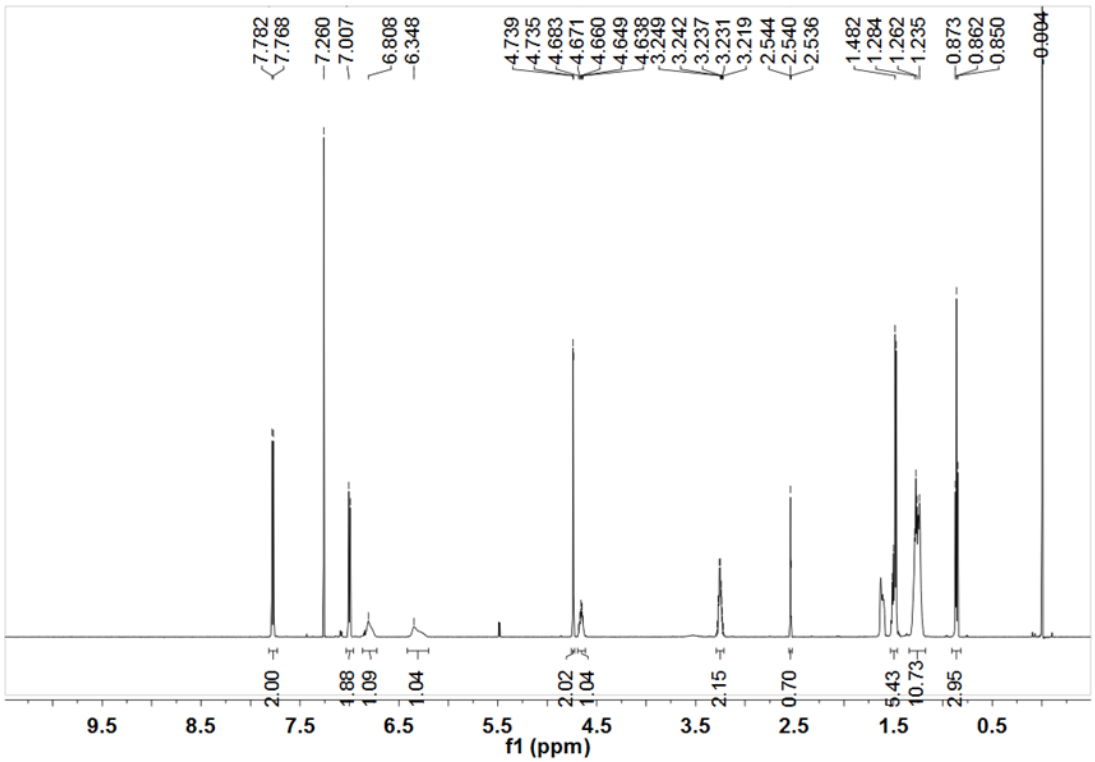

Figure S2. ^{1}H NMR spectrum of compound $\mathbf{1^{D}}$ (600 MHz) in $CDCl_3$ (5 mM).

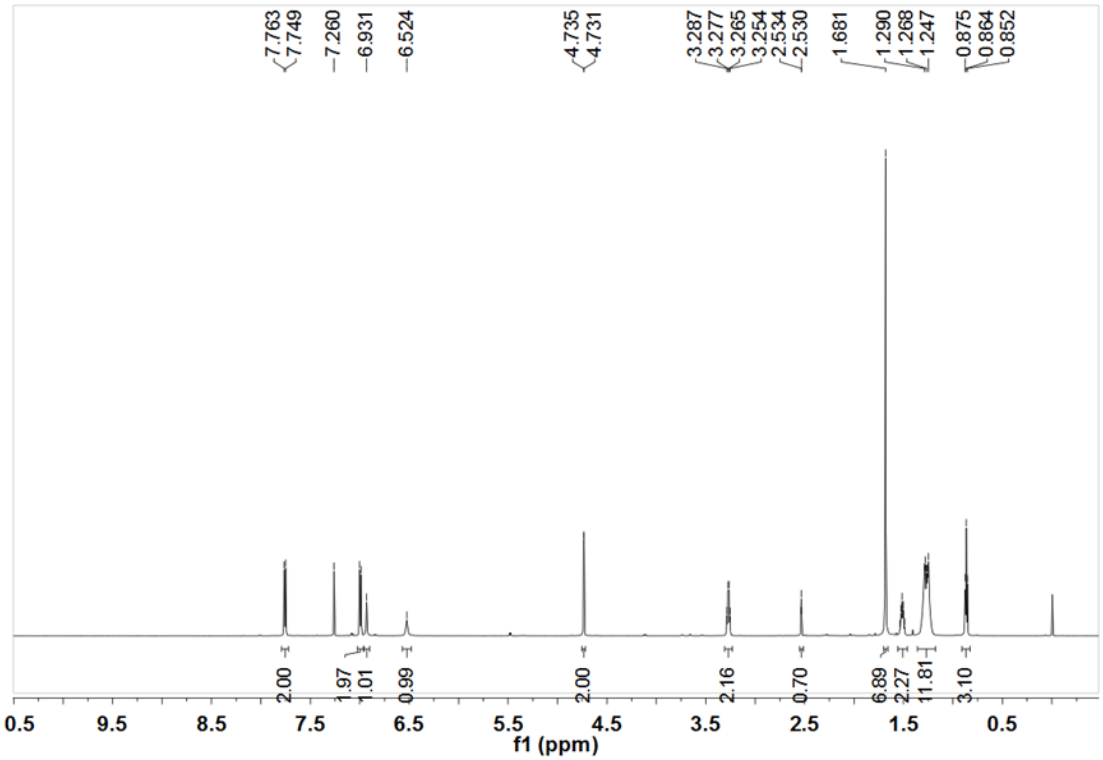

Figure S3. ^{1}H NMR spectrum of compound $\mathbf{1}^{\mathbf{A}}$ (600 MHz) in $CDCl_3$ (10 mM).

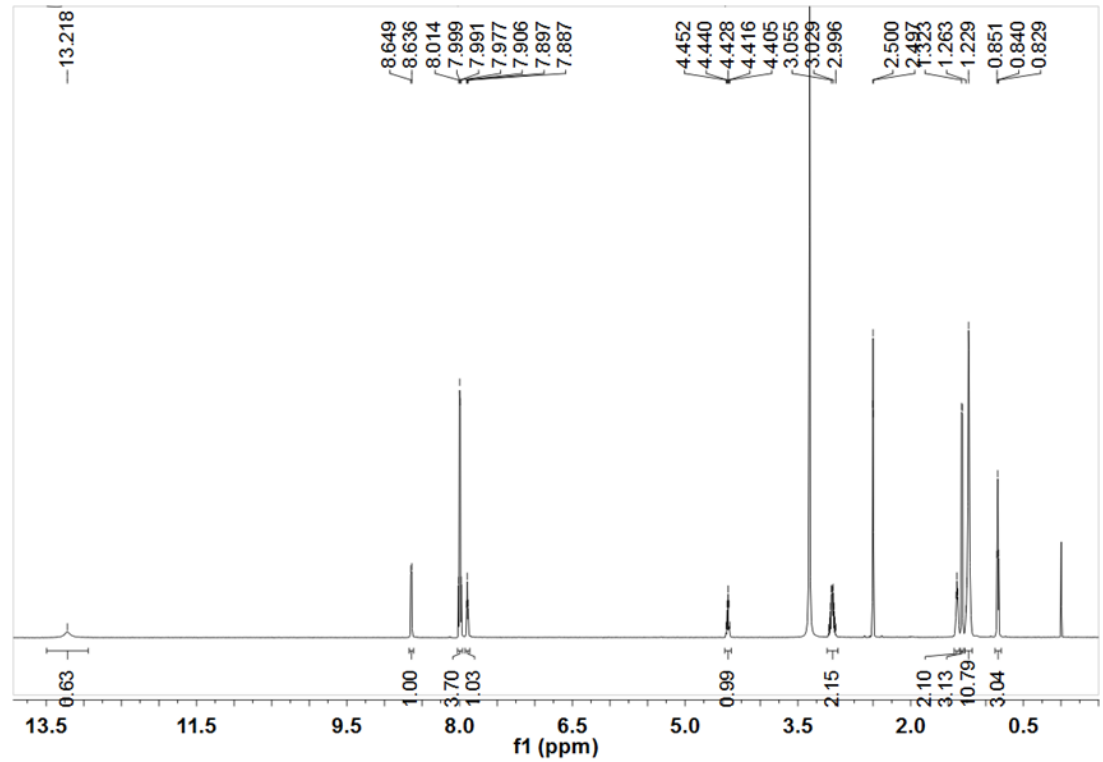

Figure S4. ^{1}H NMR spectrum of compound $\mathbf{9}^{\mathbf{L}}$ (600 MHz) in DMSO-d_6 (10 mM).

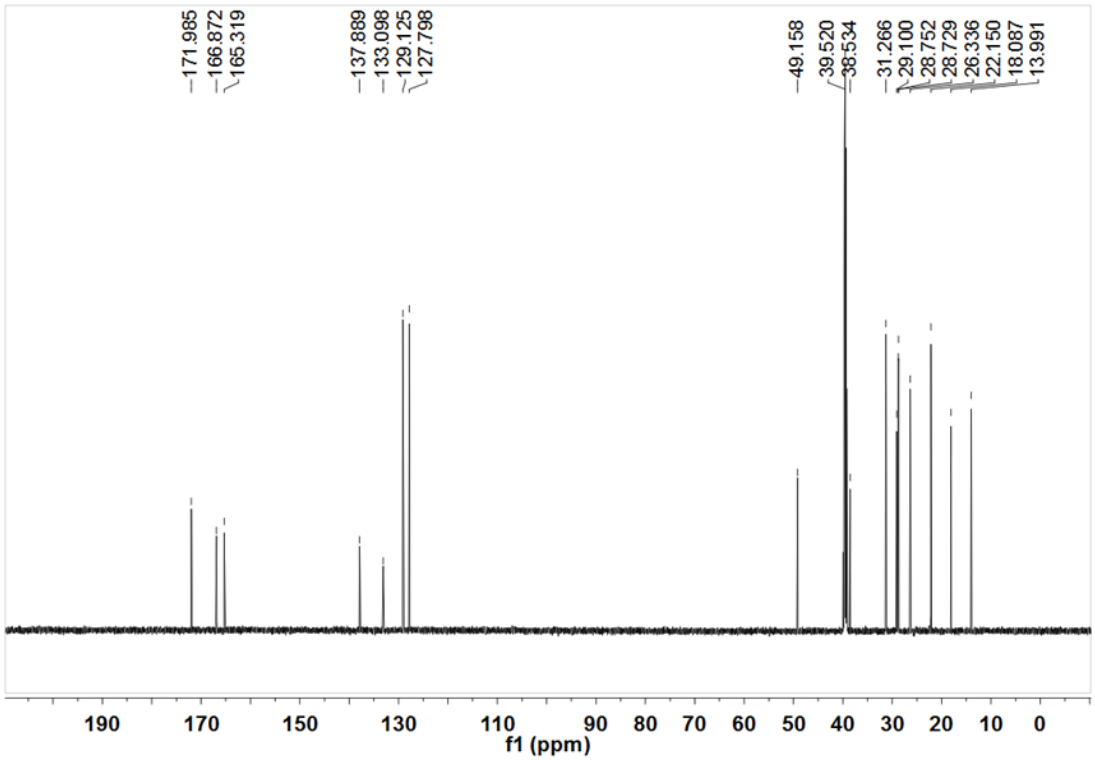

Figure S5. ^{1}H NMR spectrum of compound $\mathbf{9^{L}}$ (150 MHz) in DMSO-d_6 (10 mM).

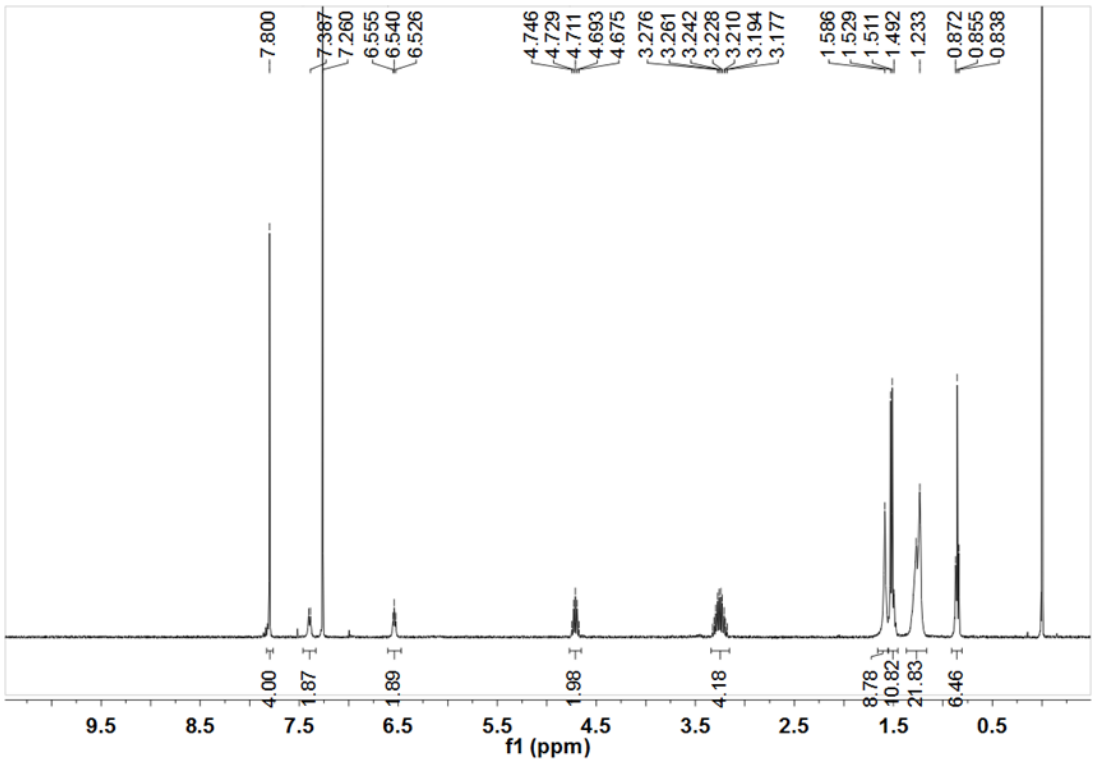

Figure S6. ^{1}H NMR spectrum of compound $\mathbf{2^{L,L}}$ (400 MHz) in $CDCl_3$ (2 mM).

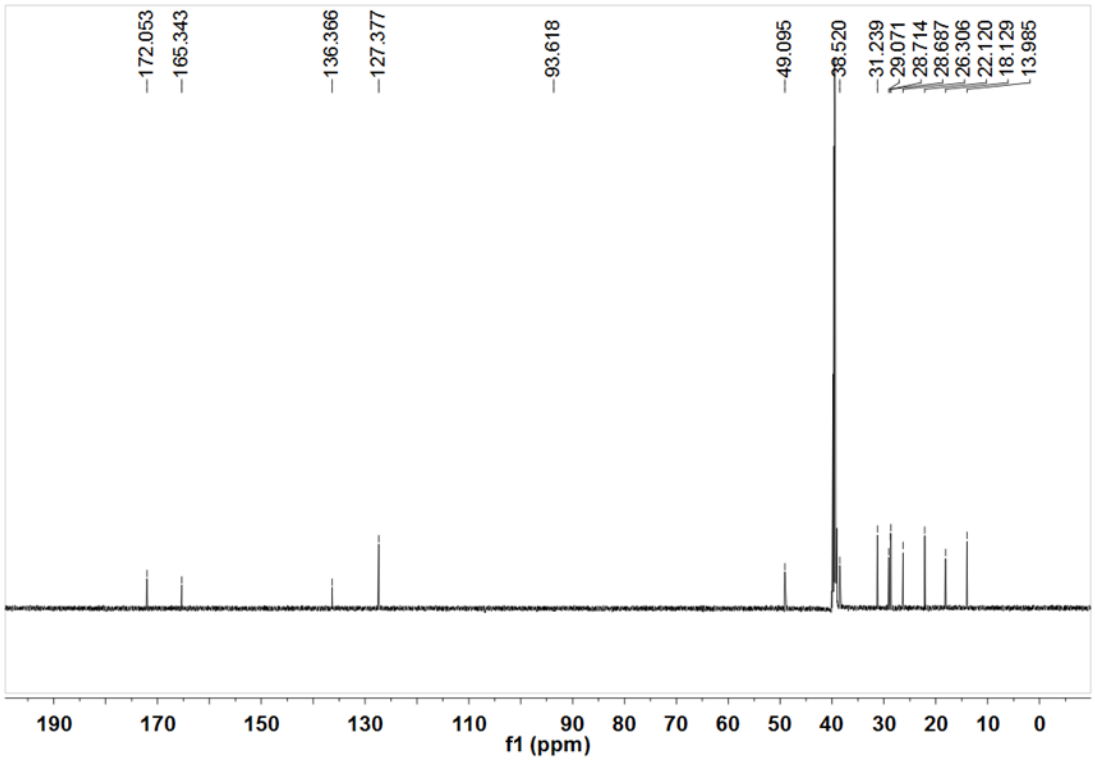

Figure S7. ^{1}H NMR spectrum of compound $\mathbf{2}^{\mathbf{L,L}}$ (150 MHz) in DMSO-d_6 (30 mM).

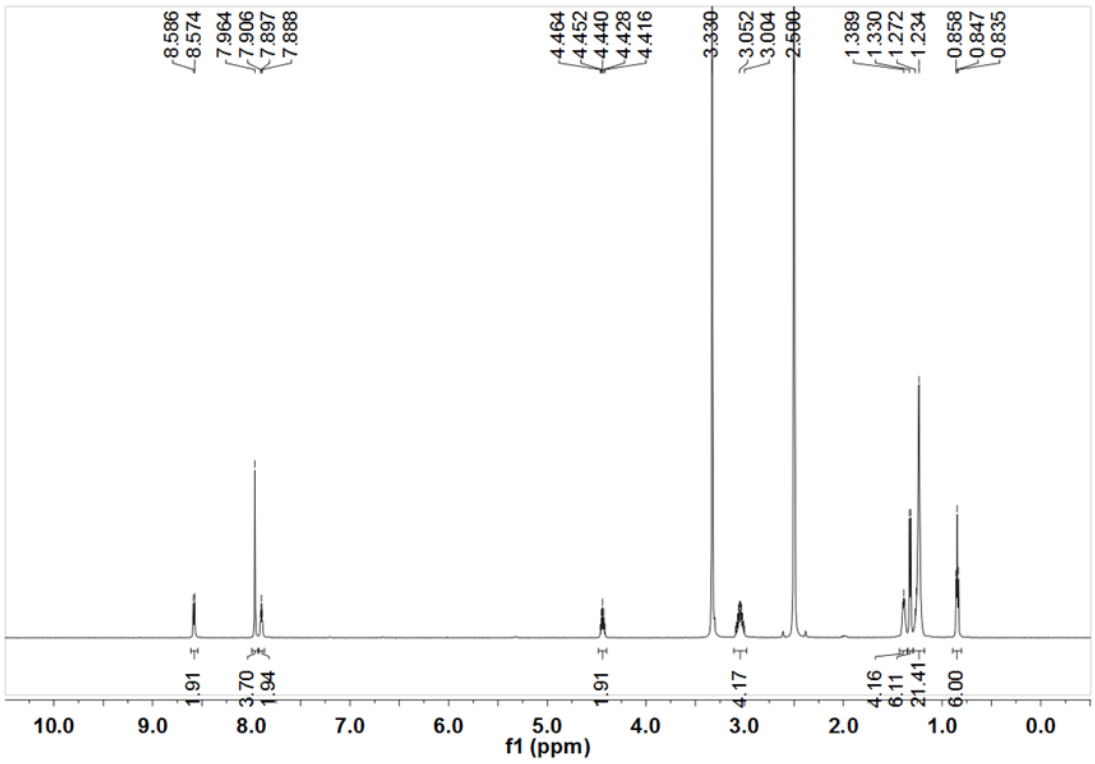

Figure S8. ^{1}H NMR spectrum of compound $\mathbf{2}^{\mathbf{D,L}}$ (600 MHz) in DMSO-d_6 (10 mM).

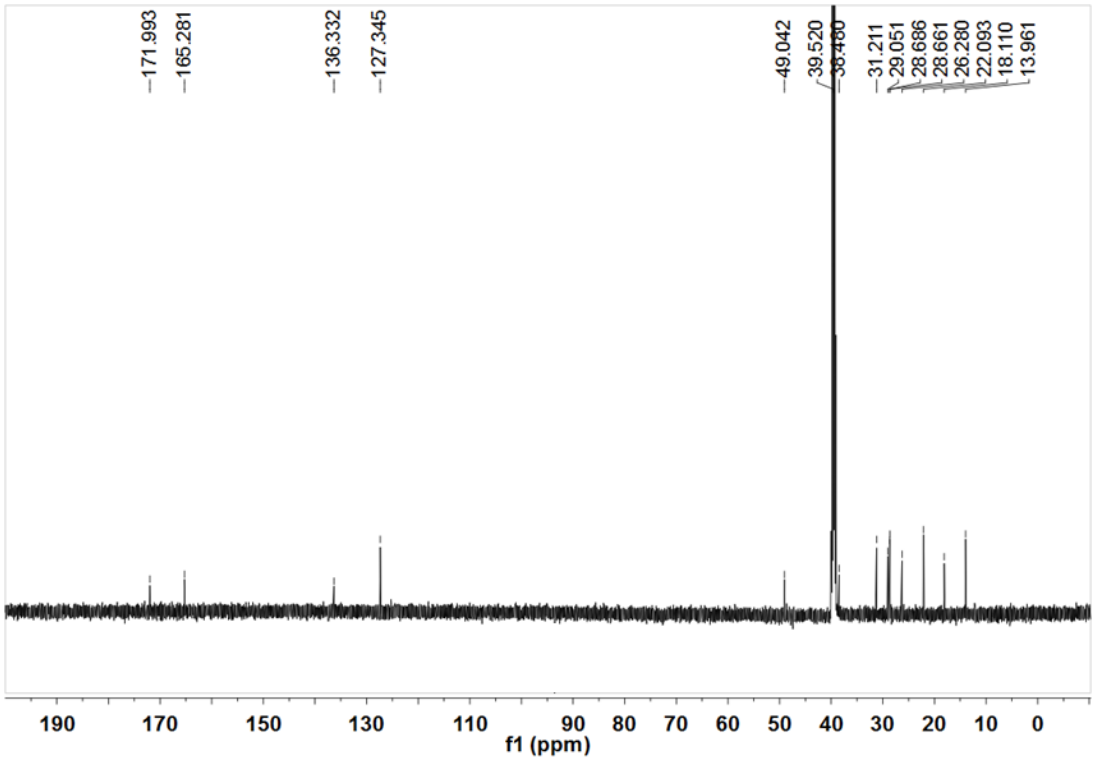

Figure S9. ^{13}C NMR spectrum of compound $\mathbf{2}^{\mathbf{D,L}}$ (150 MHz) in DMSO-d_6 (30 mM).

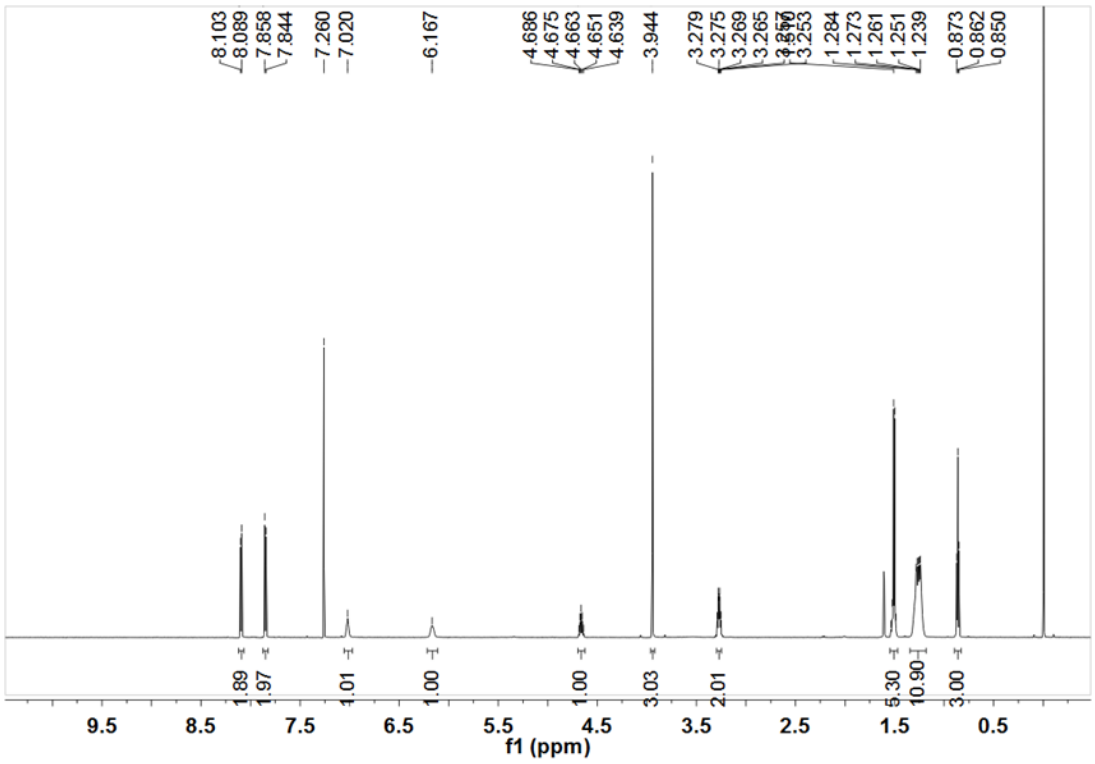

Figure S10. ^{1}H NMR spectrum of compound $\mathbf{3}^{\mathbf{L}}$ (600 MHz) in $CDCl_3$ (10 mM).

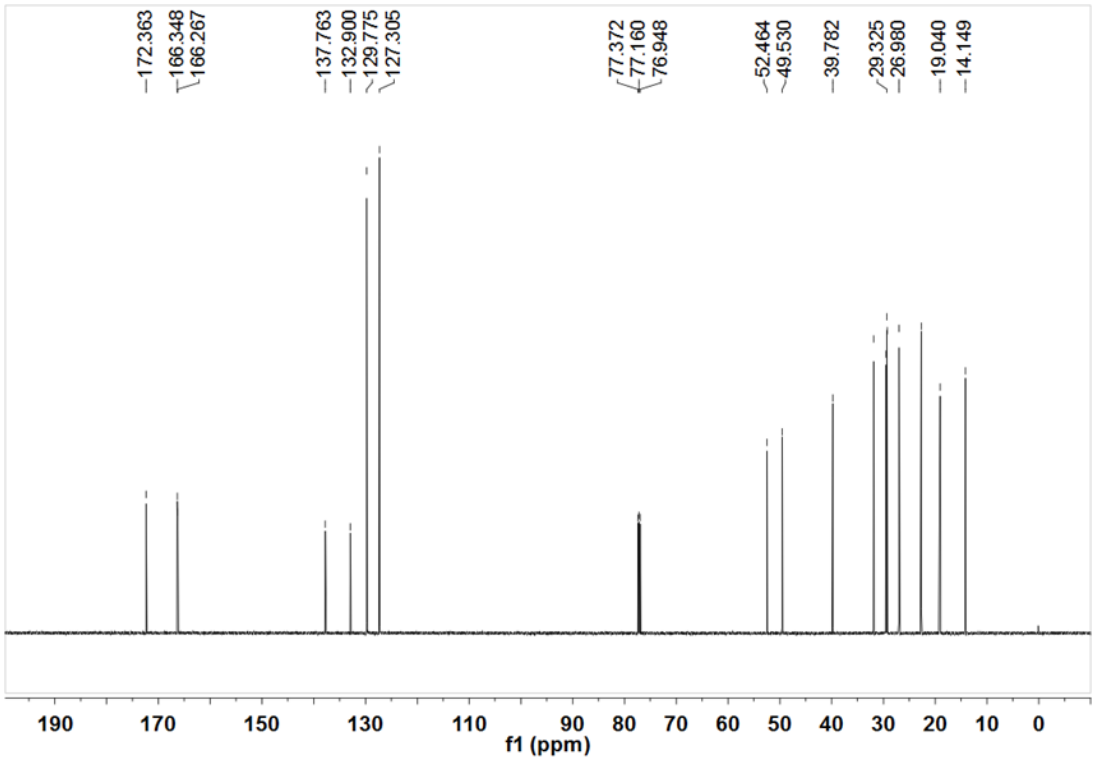

Figure S11. ^{13}C NMR spectrum of compound $\mathbf{3^L}$ (150 MHz) in $CDCl_3$ (50 mM).

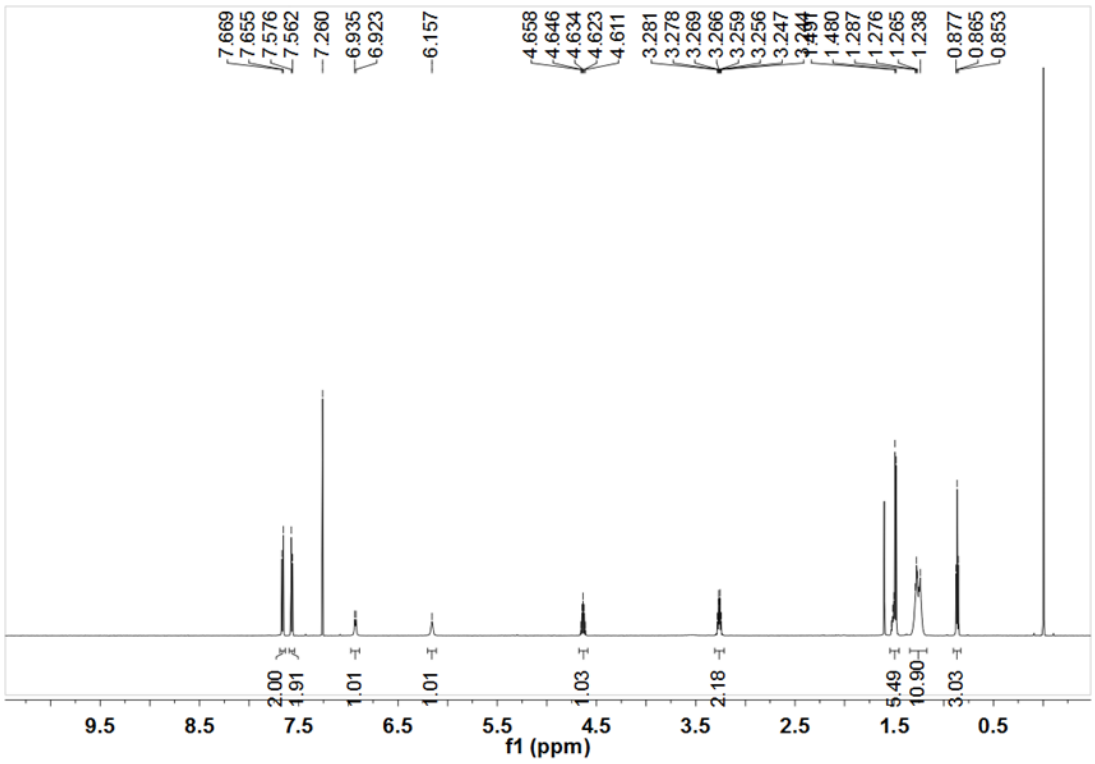

Figure S12. ^{1}H NMR spectrum of compound $\mathbf{4^L}$ (600 MHz) in $CDCl_3$ (10 mM).

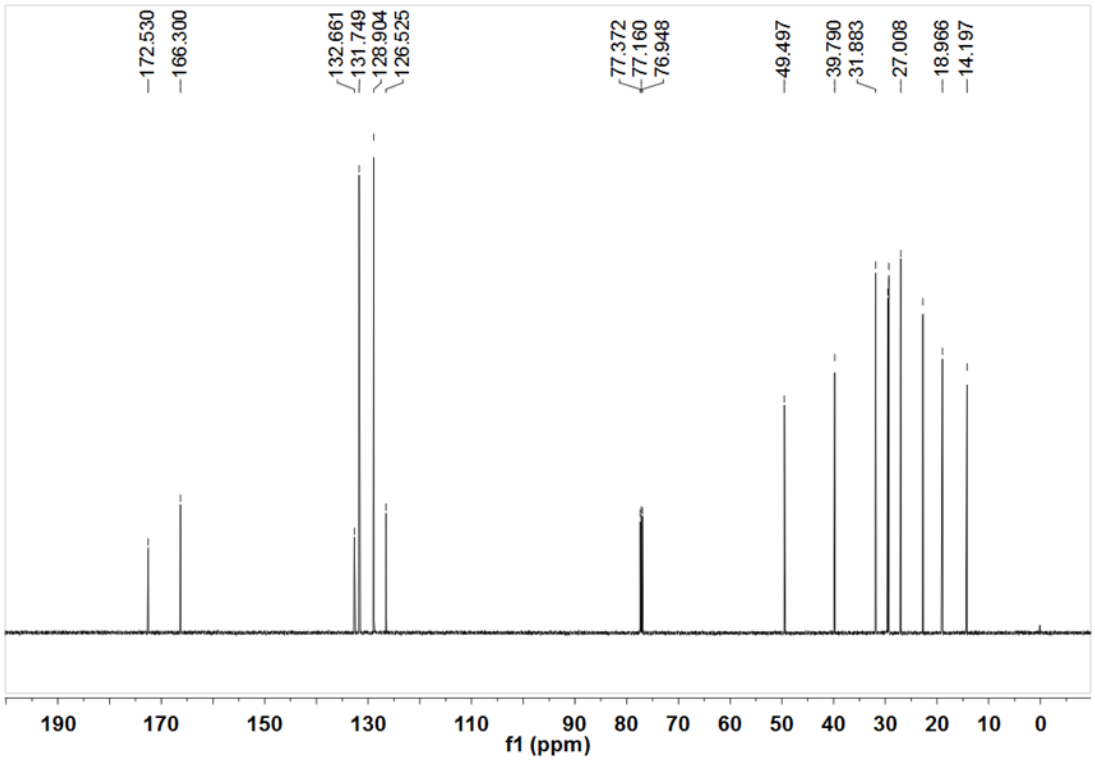

Figure S13. ^{13}C NMR spectrum of compound $\mathbf{4^L}$ (150 MHz) in $CDCl_3$ (50 mM).

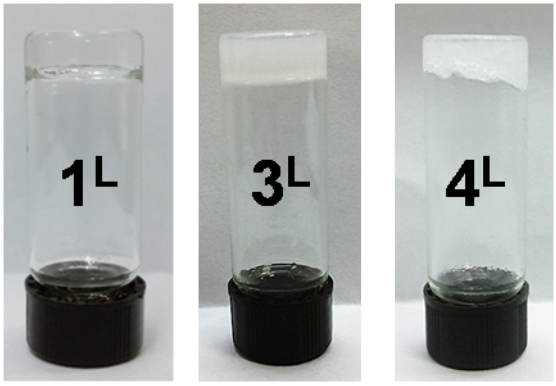

Figure S14. The organogel of $\mathbf{1^L}$ (2.0% wt), $\mathbf{3^L}$ (1.4% wt), and $\mathbf{4^L}$ (1.0% wt) in toluene.

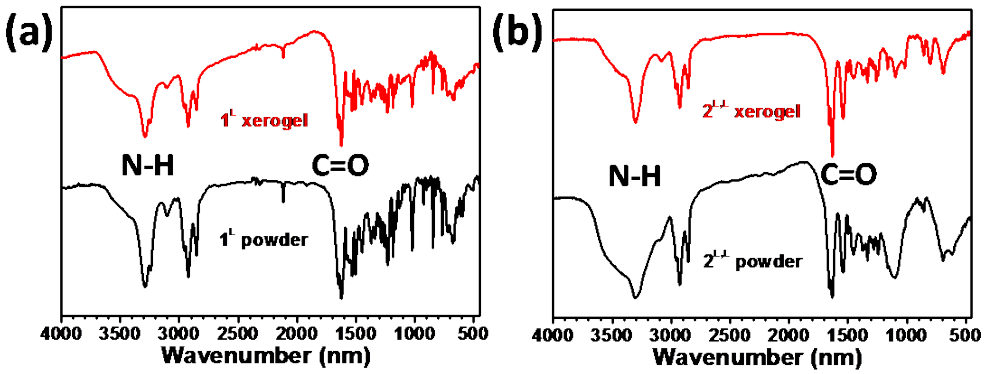

Figure S15. FT-IR spectra of powdered and xerogel samples of $\mathbf{1}^{\mathbf{L}}$ and $\mathbf{2}^{\mathbf{L,L}}$ (KBr pallet, 25 °C).

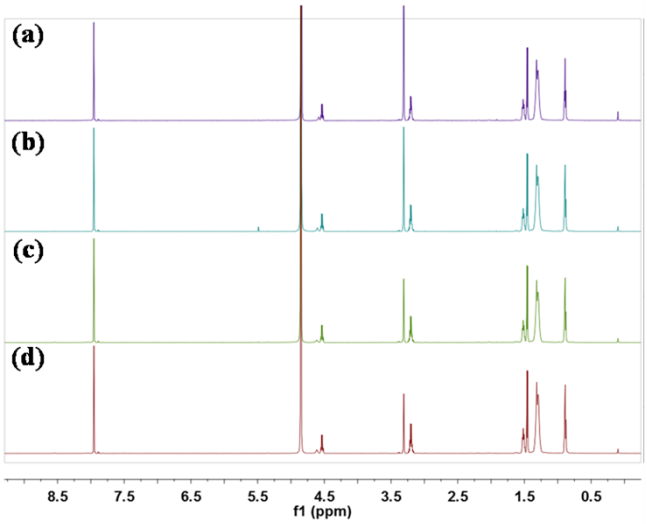

Figure S16. Partial ^{1}H NMR spectra (600 MHz) of $\mathbf{2}^{\mathbf{L,L}}$ in methanol-d_4 with different concentrations. (a) 0.01 M (0.73% wt); (b) 0.02 M (1.5% wt); (c) 0.03 M (2.2% wt); and (d) 0.04 M (2.9% wt). When the concentration of $\mathbf{2}^{\mathbf{L,L}}$ is 0.03 M and 0.04 M, opaque organogel forms in the NMR tube.

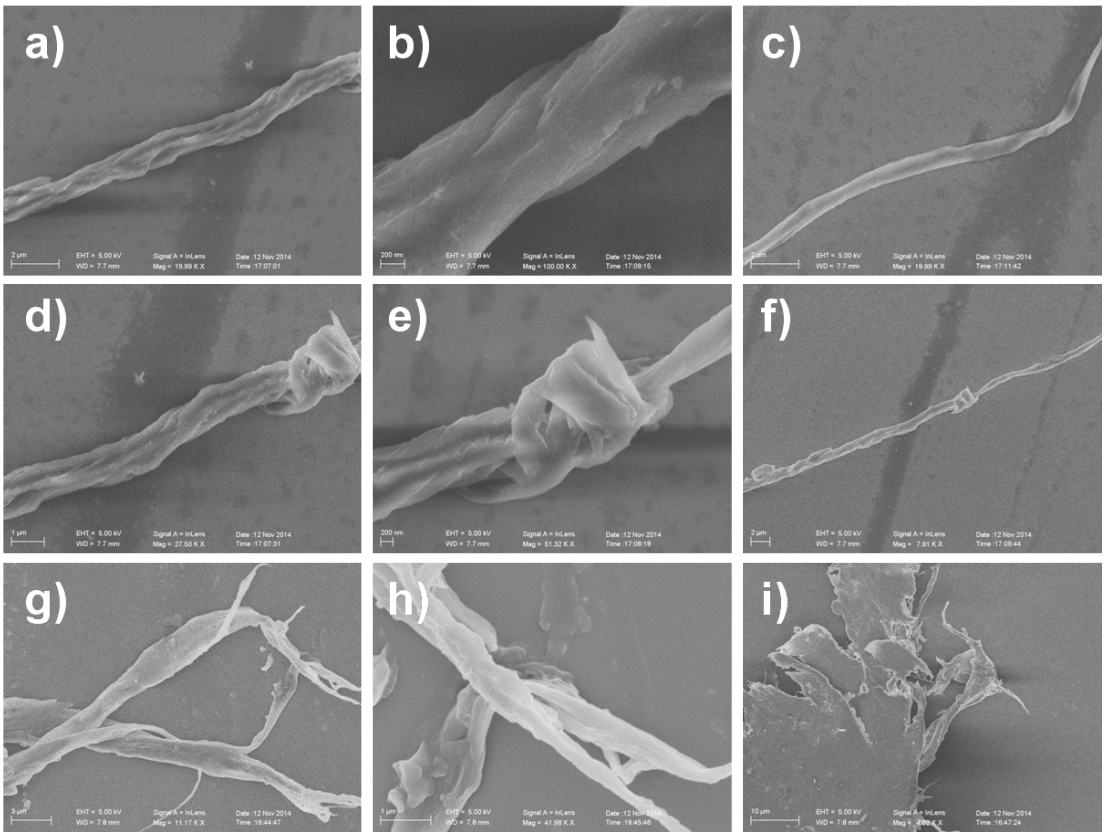

Figure S17. SEM images of chiral helix fibers obtained from the xerogel of $\mathbf{2}^{\mathbf{L,L}}$ in dichloroethane.

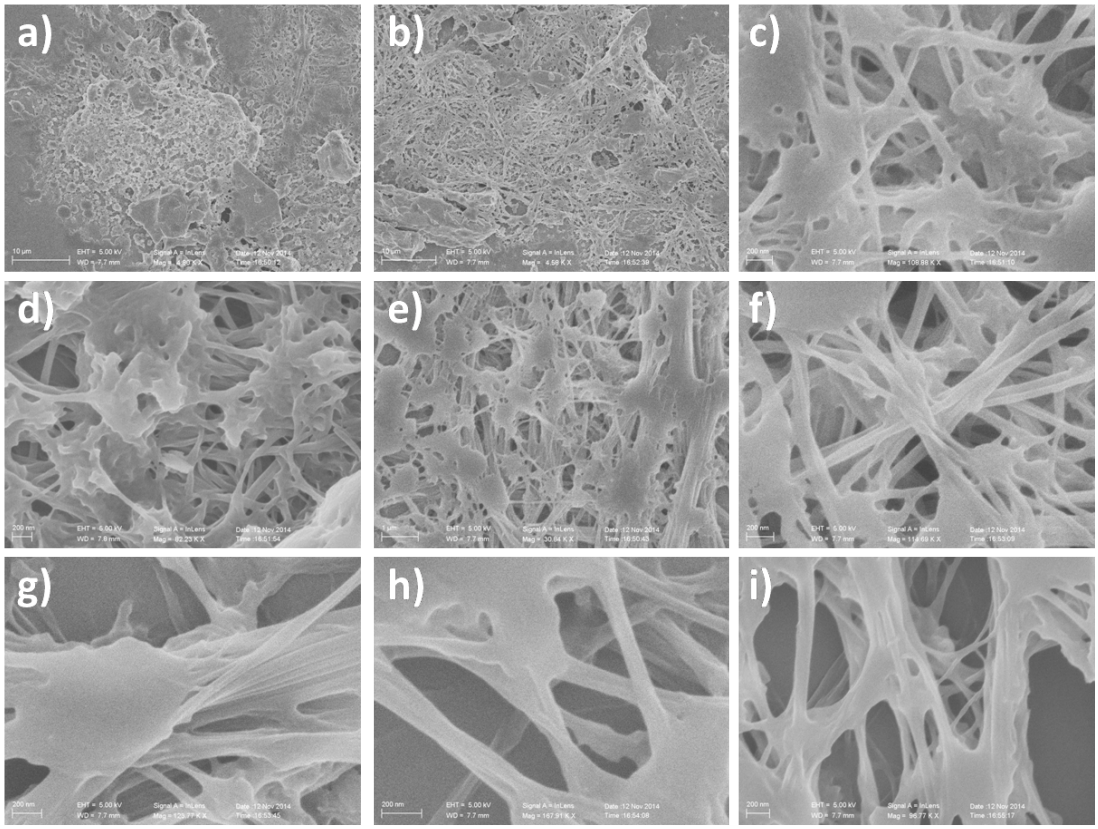

Figure S18. SEM images of chiral helix fibers obtained from the xerogel of $\mathbf{2}^{\mathbf{L,L}}$ in ethanol.

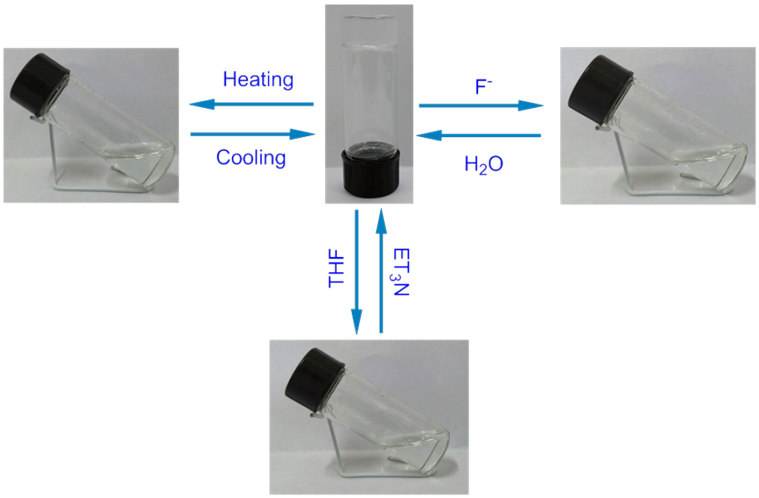

Figure S19. The multi-stimuli-responsiveness behaviour of gel of $\mathbf{2}^{\mathbf{L,L}}$ in toluene by thermal, pH value, and floride ion.

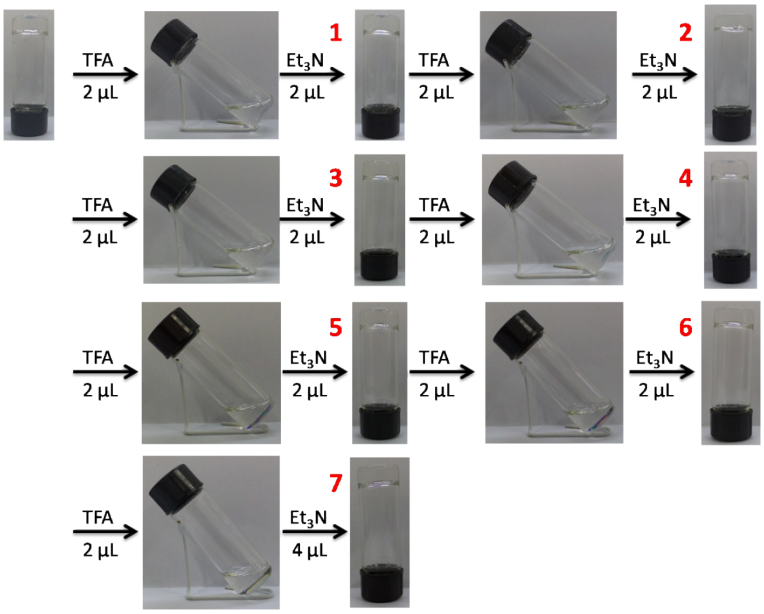

Figure S20. The transition cycle repeated for seven times when acid (TFA) and base (Et_3N) were added alternately. In the seventh cycle, 2.0 equivalent of Et_3N was needed to reform the gel.

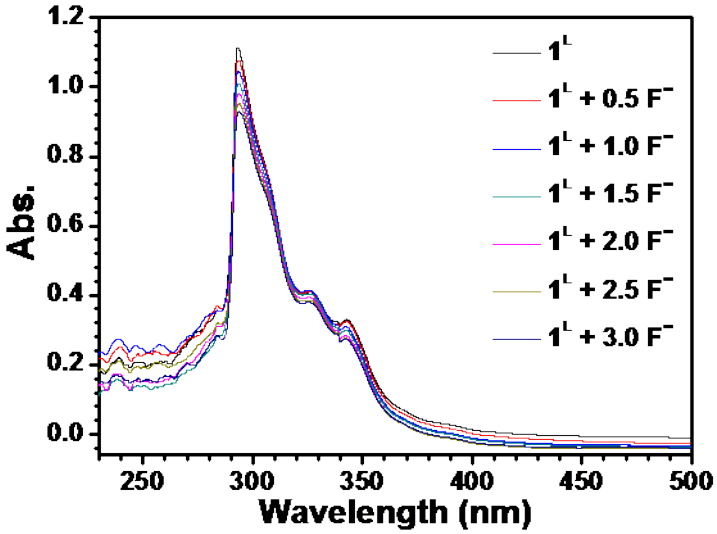

Figure S21. UV-vis titration of $\mathbf{1^L}$ (5×10^{-5} M) with *n*-Bu_4NF in *o*-dichlorobenzene solution.